

Title page

Title

A semi-physiological population model for prediction of the pharmacokinetics
of drugs under liver and renal disease conditions

Authors

Ashley Strougo,

Ashraf Yassen,

Walter Krauwinkel,

Meindert Danhof,

Jan Freijer

Affiliation

AS, AY, WK, JF

Global Clinical Pharmacology & Exploratory Development, Astellas Pharma
Europe, Leiderdorp, The Netherlands

AS, MD

Division of Pharmacology, Leiden/Amsterdam Center for Drug Research,
Leiden University, Leiden, The Netherlands

Running title page

Running title

A semi-physiological approach for predicting pharmacokinetics

Corresponding author

Ashley Strougo

Global Clinical Pharmacology & Exploratory Development

Astellas Pharma Global Development Europe

Elisabethhof, 1 2353 EW Leiderdorp The Netherlands

P.O.Box 108, 2350 AC Leiderdorp The Netherlands

Tel: +31 71 545 5069

Mob: +31 6 2040 0688

Fax: +31 71 545 5276

E-mail: ashley.strougo@eu.astellas.com

Number of text pages: 20

Number of tables: 6

Number of figures: 6

Number of references: 33

Number of words in the abstract: 249

Number of words in the introduction: 677

Number of words in the discussion: 1234

List of non-standard abbreviations

AGP α 1-acid glycoprotein

C_{AGP} AGP-plasma concentration

$C_{Albumin}$ Albumin-plasma concentration

CL Clearance

CL_H Hepatic clearance

$CL_{in\ vitro}$ in vitro clearance

$CL_{in\ vivo}$ in vivo clearance

CL_{int} Intrinsic clearance

CL_R Renal clearance

F_{max} Maximum oral bioavailability

f_{tissue} Free fraction in tissue

f_u free-fraction in plasma

GFR glomerular function ratio

k_{AGP} Partition coefficient for AGP

$k_{Albumin}$ Partition coefficient for albumin

NSB non-specific binding

Q Inter-compartmental clearance

Q_H Liver blood flow

V_1 Central volume

V_{plasma} Plasma volume

V_{SS} volume of distribution

V_{water} Aqueous volume outside of the plasma

WB-PBPK whole-body physiologically based pharmacokinetic model

Abstract

The application of model-based drug development in special populations becomes increasingly important for clinical trial optimization, mostly by providing rationale for dose selection and thereby aiding risk-benefit assessment. In this paper, a semi-physiological approach is presented enabling the extrapolation of the pharmacokinetics from healthy subjects to patients with different disease conditions. This semi-physiological approach was applied to solifenacin, using clinical data on total and free plasma and urine concentrations in healthy subjects. The analysis was performed using non-linear mixed effect modeling and relied on the utilization of a general partitioning framework to account for binding to plasma-proteins and to non-plasma tissues together with principles from physiology that apply to the main pharmacokinetic process, i.e., bioavailability, distribution and elimination. These physiology principles applied allowed quantification of the impact of key physiological parameters (i.e., body composition, glomerular function, liver enzyme capacity and liver blood flow) on the pharmacokinetics of solifenacin. The prediction of the time course of the drug concentration in liver and renal impaired patients only required adjustment of the physiological parameters that are known to change upon liver and renal dysfunction without modifying the pharmacokinetic model structure and/or its respective parameter estimates. Visual predictive checks showed that the applied approach was able to adequately predict the pharmacokinetics of solifenacin in liver and renal impaired patients. Also, a better insight into the pharmacokinetic properties of solifenacin was obtained. In conclusion, the proposed semi-

physiological approach is attractive for prediction of altered pharmacokinetics of compounds influenced by liver and renal disease conditions.

Introduction

Disease conditions can imply important alterations in drug disposition, metabolism and/or absorption when compared with healthy subjects. In liver and renal impairment, the main alterations are caused by changes in organ blood flow and plasma protein binding that affect the intrinsic capacity of the organ to metabolize/excrete drugs. Such physiological changes may affect the pharmacokinetics of drugs. Therefore, the pharmacokinetics of drugs that are likely to be administered under these pathological conditions should be assessed in clinical studies to provide alternative dosing recommendations. Model-based analysis and simulation is invaluable in optimization of these clinical studies mostly by providing a rationale for dose selection, thereby avoiding side-effects due to unexpectedly high exposure of the drug. Accordingly, this approach aids risk- benefits assessment of dose selection.

The impact of altered liver function on the pharmacokinetics of a drug often depends on the stage of the disease, which occurs through different pathological mechanisms. Some of the known physiological changes that can affect the pharmacokinetics are shunting of blood past the liver, impaired hepatocellular function, impaired biliary excretion and decreased plasma protein binding (Schuppan and Afdhal 2008). The impact of enzyme activities, plasma-protein concentration and hepatic blood flow (portal plus arterial) on the clearance (CL) of different compounds has been previously characterized according to the Child-Pugh score classification and using well-stirred models (Edginton and Willmann 2008; Johnson *et al.* 2010).

Reduction in liver function can also be caused by reduction in renal function. To this end, the pharmacokinetics of drugs that are mainly metabolized by the liver can be markedly affected by renal impairment. Chronic renal disease influences not only GFR, tubular secretion and protein binding but also has an impact on intestinal and hepatic uptake transporters (Nolin *et al.* 2008). Briefly, the reduction of renal clearance leads to accumulation of uremic toxins and chronic inflammation, which then perturbs metabolic and transport processes in the liver and intestine (Dreisbach 2009). For end-stage renal disease, dialysis removes the uremic factors (Dreisbach 2009) and consequently patients with severe renal impairment, who are not yet on dialysis are in theory at the highest risk for having higher drug exposure than end-stage renal disease patients.

Model-based pharmacokinetic analysis can be used to gain more insights in how (patho-) physiological changes can impact the pharmacokinetics of a compound. To date, whole-body physiologically based pharmacokinetic (WB-PBPK) models have been proposed in two previously published reports for prediction of the pharmacokinetics in patients with liver impairment (Edginton and Willmann 2008; Johnson *et al.* 2010). WB-PBPK requires a large number of physiological input parameters and well understanding of all active processes affecting the pharmacokinetic properties of a drug. Thus, the lack of sufficient *in-vitro* and *in-vivo* data may hamper the use of this approach. In this investigation, we propose an approach which takes into account key principles from physiology in combination with the power of the non-linear mixed effect modelling for estimation of population and random-effect parameters.

This semi-physiological population approach is proposed to predict the pharmacokinetics from healthy subjects to patients with two different disease conditions, i.e., renal and liver impairment. This approach combines an empirical compartmental model structure, a partitioning framework to describe protein binding in plasma and principles of the physiology that apply to volume of distribution (V_{SS}) and CL in order to determine the impact of key physiological parameters (i.e., free-fraction in plasma (f_u), total body water composition, liver weight, liver blood flow (Q_H) and glomerular filtration rate (GFR)) on the pharmacokinetic profiles.

The clinical utility of the proposed approach is illustrated with solifenacin (YM905; Vesicare[®]), which is a once-daily orally administered selective muscarinic (M_1 and M_3) receptor antagonist for the treatment of overactive bladder (Payne 2006; Simpson and Wagstaff 2005). Solifenacin is primarily metabolized by the cytochrome P450 3A4 isozyme (CYP3A4) leading to roughly 7% of the dose being excreted unchanged in the urine (Doroshenko and Fuhr 2009; Michel *et al.* 2004). Further, solifenacin exhibits a dose-proportional pharmacokinetics and extensively binds to α_1 -acid glycoprotein (AGP) and to a lesser extent to albumin, which makes it a suitable model compound to investigate the utility of the proposed semi-physiological approach.

Methods

Clinical studies

An overview of the clinical studies used for model development and comparison with model predictions is shown in Table I. In total, the data of 59 subjects of three phase I clinical studies after administration of 5 mg and 10 mg of solifenacin were used for model development including data of young healthy male adults, young healthy female adults, elderly females and elderly males. The data from 26 patients with liver and renal impairment were exclusively used to verify the model predictions. In total, data of approximately 8 patients with liver impairment and 6 patients with renal impairment was available for each group. Patients with liver impairment included in study 2 were classified as type B in the Child Pugh category and patients with renal impairment were classified as mild ($\text{GFR} \geq 50$ and < 80 mL/min), moderate ($\text{GFR} \geq 30$ and < 50 mL/min) or severe ($\text{GFR} < 30$ mL/min). For the patient classification, GFR was calculated according to Cockcroft-Gault equation (Cockcroft and Gault 1976). Solifenacin concentrations were in all studies analyzed using liquid chromatography/mass spectrometry (HPLC-MS) with a limit of quantification of 1.38 nmol/L for total-solifenacin and 0.55 nmol/L for free-solifenacin. The comprehensive description of these studies and results has been reported elsewhere (Krauwinkel *et al.* 2005; Kuipers *et al.* 2006; Smulders *et al.* 2007).

Structural model

The structural model to describe the pharmacokinetics of solifenacin is shown in Figure 1. Briefly, the biphasic pharmacokinetics of total and free solifenacin

in plasma was described by a two compartment model with first-order absorption. The urine concentrations were described by linking the urinary excretion to the central compartment. To account for the effect of protein binding on the central volume of distribution (V_1), the central compartment of this system was assumed to have different components that are in instantaneous equilibrium: solifenacin-AGP, solifenacin-albumin, solifenacin-free and solifenacin-non-specific binding (NSB) (Figure 1). NSB was assumed to be outside of the plasma so that variations in the concentration of plasma-proteins would have an effect on the total-solifenacin plasma concentrations. The higher the concentration of plasma-proteins, the less solifenacin distributes from plasma to the NSB and consequently the higher the total-solifenacin concentrations are observed in plasma.

By applying the “law of mass action” to the plasma distribution component, the f_u could be defined as:

$$f_u = \frac{1}{1 + \frac{C_{AGP}}{k_{AGP}} + \frac{C_{Alb}}{k_{Alb}}} \quad (1)$$

in which C_{AGP} is the AGP-plasma concentration, C_{Alb} is the albumin-plasma concentration, k_{AGP} is the partition coefficient for AGP and k_{Alb} is the partition coefficient for albumin.

To describe the V_1 the following equation was derived:

$$V_1 = V_{\text{plasma}} \cdot (1 + \beta \cdot f_u) \quad (2)$$

where β represents a compilation of the concentration in the NSB divided by the partition coefficient for NSB and V_{plasma} is the volume of plasma

calculated as 5 percent of the lean body mass (Boer 1984;Janmahasatian *et al.* 2005).

In addition, the effect of f_u on V_{SS} was included into the model by taking into account its physiological determinants (Gibaldi and McNamara 1978;Mehvar 2005):

$$V_{SS} = V_{\text{plasma}} + V_{\text{water}} \cdot \left(\frac{f_u}{f_{\text{tissue}}} \right) \quad (3)$$

in which f_{tissue} is the free fraction in tissue and V_{water} is the aqueous volume outside of the plasma into which the drug distributes (Rowland and Tozer 1995). Hence, V_{water} was assumed to be total body water composition *minus* plasma water volume, which is approximately 90% of V_{plasma} . Total body water composition was calculated according to Watson *et al* (Watson, Watson, and Batt 1980).

The simultaneous analysis of the solifenacin plasma and urine concentrations enable the characterisation of both renal clearance (CL_R) and hepatic clearance (CL_H) as illustrated in equation (4).

$$CL = CL_R + CL_H \quad (4)$$

Renal clearance has been characterised as a fraction of the clearance due to the glomerular filtration rate (CL_{GFR}) as displayed in equation (5).

$$\begin{aligned} CL_R &= \alpha \cdot CL_{GFR} \\ CL_{GFR} &= GFR \cdot f_u \end{aligned} \quad (5)$$

Where α is a fraction of CL_{GFR} . If $\alpha > 1$, tubular active secretion is mainly involved in renal clearance; if $\alpha < 1$ reabsorption is mainly involved in renal clearance; and if $\alpha = 1$ GFR is sufficient to explain all renal clearance. GFR was calculated according to the modification of diet in renal disease (MDRD) equation (Levey *et al.* 1999) and corrected for body surface area (Haycock, Schwartz, and Wisotsky 1978).

In order to characterise the CL_H , the well-stirred model concept was included into the model according to equation (6) (Yang *et al.* 2007).

$$CL_H = \frac{Q_H \cdot f_u \cdot CL_{int}}{Q_H + f_u \cdot \frac{C_{int}}{C_{blood}/C_{plasma}}} \quad (6)$$

where Q_H was calculated according to Wynne *et al.* (Wynne *et al.* 1989); C_{blood}/C_{plasma} is total blood plasma concentration ratio which was fixed at 0.89 as *in vitro* established (results not published); and CL_{int} is intrinsic clearance which was calculated as follows:

$$CL_{int} = CL_{in vivo} \cdot \text{liver weight} \cdot \text{MPPGL} \quad (7)$$

where $CL_{in vivo}$ is the *in vivo* clearance, liver weight was calculated according to Chouker *et al.* (Chouker *et al.* 2004) and MPPGL is the milligrams of microsomal protein per gram liver which adult levels were reported as 35 mg/g (Johnson, Rostami-Hodjegan, and Tucker 2006).

Inter-compartmental clearance (Q) of solifenacin was assumed to be dependent on f_u (equation (8))

$$Q = Q^* \cdot f_u \quad (8)$$

in which Q^* was a model constant.

Maximal oral bioavailability (F_{\max}) was physiologically characterized in this model as described in equation (9)

$$F_{\max} = \frac{Q_H}{Q_H + CL_{\text{int}}} \cdot \frac{f_u}{C_{\text{blood}} / C_{\text{plasma}}} \quad (9)$$

Table II shows an overview of the demographic covariates necessary to calculate the physiological parameters and consequently to derive model parameters.

Random effects

Random inter-individual variability on each pharmacokinetic parameter was perceived as a log-normal distribution (equation (10)).

$$P_i = P_{\text{typical}} \cdot \exp(\eta_i) \quad (10)$$

where P_i represents the parameter value for the i^{th} individual, P_{typical} is the parameter for a typical group value and η is the inter-individual random effect with $\eta_i \sim N(0, \sigma^2)$.

The residual errors were separately defined for total and free-solifenacin concentration in plasma and solifenacin concentration in urine:

$$C_{\text{obs}, ij} = C_{\text{pred}, ij} \cdot (1 + \varepsilon_{ij}) \quad (11)$$

where $C_{\text{obs},ij}$ and $C_{\text{pred},ij}$ are respectively the observed concentration and the predicted concentration in individual i at time j and ε_{ij} is the residual error with $\varepsilon_i \sim N(0, \sigma^2)$.

Model performance

Throughout model development NONMEM subroutine ADVAN6 and first order conditional estimation with interaction was used. Samples below limit of quantification were considered as missing values. Model performance was evaluated by both visual inspection and likelihood ratio test. Physiological considerations and the conventional critical values for the likelihood ratio test ($p < 0.001$) were used for model development. Precision of parameter estimates was evaluated as coefficient of variation (CV) calculated by the ratio of the estimated standard error and its respective parameter estimate multiplied by 100.

Model evaluation

Internal model validation was performed by means of a visual predictive check, which evaluates whether the identified model is able to predict the observed total plasma concentrations, urine excretion rates and f_u (Post *et al.* 2008). Plasma concentration-time, urine excretion rate-time and f_u -plasma protein curves were simulated for 1000 hypothetical subjects. In all simulations, correlation matrix for theta estimates was considered to account for parameter uncertainty.

For the simulation of plasma concentration and urine excretion rate curves, the physiological parameters (i.e. V_{plasma} , V_{water} , Q_H , liver weight and GFR)

were calculated by sampling the required demographic covariates and the plasma-protein concentrations (i.e., AGP-plasma concentration and albumin-plasma concentration) from the data set used for model development. For the simulations of f_u -AGP curve, albumin-plasma concentration was fixed to the average value observed in the data set and AGP-plasma concentration was allowed to vary within the observed range. The opposite was applied for the simulations of f_u -albumin curve.

Graphical representation of total plasma and urine data show 90% predicted population variability explained by the differences in the physiological parameters alone (inner shade) and combined with the estimated inter-individual variability (outer shade). For graphical representation of urine data, urine excretion rate was calculated by dividing the simulated amount of total-solifenacin excreted in the urine during a certain time-interval by the time interval. Graphical display of f_u shows 95% confidence interval of the population median. The observed f_u was calculated by dividing free-solifenacin by total-solifenacin plasma concentrations per time point.

Extrapolations

The model developed for the healthy subjects was subsequently used to extrapolate the pharmacokinetics in plasma and urine to patients with liver and renal impairment. For the extrapolations, the data in patients was compared with the model predictions, which were exclusively based on the alterations of the physiological parameters. In order to evaluate to which extent the identified model is able to predict the plasma and urine data in these pathological conditions, a visual predictive check of the full

pharmacokinetic profiles was performed. A posterior predictive check of V_{SS} , CL and renal clearance was performed to characterize the possibility that the pharmacokinetic parameter predictions are in accordance with the limited amount of patients recruited for the clinical studies.

The visual predictive check was performed in a similar way as for the model evaluation. The physiological alterations were considered by using literature reported values (Table III) and by using the observed physiological parameters (Table IV). Alterations in Q_H and intrinsic clearance were in both cases assumed to be as reported in the literature. Graphical representation of plasma and urine data shows 90% predicted population variability explained by alterations in the physiological parameters combined with the estimated random inter-individual variability in healthy subjects (shade).

For the posterior predictive check, only the observed alterations in the physiological parameters (Table IV) were used to predict V_{SS} , CL and renal clearance. In total, 1000 data sets for each pathological condition were simulated containing the same number of patients/samples as observed in the original data set. The 1000 simulated data sets each provided a value for the median and hence an estimate of the posterior predictive distribution. The simulated median and its 95% confidence interval were compared to the median of the observed pharmacokinetic parameters originated from a post-hoc analysis. If the medians of the post hocs were within the 95% confidence interval of the posterior predictive distribution, then the prediction was deemed plausible.

For the renal impaired patients, the fraction of 0.6 used in the extrapolations to reflect the change in intrinsic clearance is the average change in hepatic clearance between healthy subjects and severe renal impaired patients for cyclophosphamide (0.69), felbamate (0.65), roboxetine (0.44) and telithromycin (0.68) reported by Nolin *et al* (Nolin *et al.* 2008). Compounds where dialysis dependent patients were included were not considered. In this publication, severe renal impaired patients were often considered as the patients with a GFR within the range of 10 and 40 mL/min/1.73m².

Software

Nonlinear mixed effect modelling was implemented using NONMEM version 7 (GloboMax, Ellicot City, Maryland, USA). Data management and simulations were performed using R version 2.10.1 (R Foundation for Statistical Computing, Vienna, Austria).

Results

Data

Table IV compares the physiological parameters of the control group of studies 1 and 2 (Table I) to the physiological parameters of the liver impaired patients and mild, moderate and severe renal impaired patients. The median AGP-plasma concentration in the liver impaired patients was 1.6 times lower and in the severe renal impaired patients was 1.4 times higher than in the control group. Mild and moderate renal impaired patients did not show marked differences in AGP-plasma concentration. Albumin-plasma concentration was not markedly changed in liver and mild renal impaired patients and was reduced in moderate and severe renal impaired patients. GFR was shown to decrease by a factor of 0.89 in the liver impaired patients when compared with the control groups.

In renal impaired patients, GFR calculated using the MDRD equation resulted in lower GFR values than the ones using Cockcroft-Gault, which were the base for the classification of the patients as mild, moderate or severe renal impaired. For all other physiological parameters no clear differences were observed between the control groups and the liver and (mild, moderate and severe) renal impaired patients.

Structural model

The semi-physiological model to describe the effect of protein binding and key physiological parameters on the pharmacokinetics of solifenacin is illustrated in Figure 1. During model development, the equation (9) was used to calculate the bioavailability which was found to be comparable to the bioavailability

obtained in a clinical study (Kuipers *et al.* 2004). Similarity of the results allowed inclusion of F_{\max} as F into the model.

Table V displays the pharmacokinetic parameters that were estimated and derived by the final model in healthy subjects. All structural parameters were estimated with good precision (CV < 20 %). The value of f_u was 0.0205 (range 0.0139 - 0.0264), V_{SS} as 484 (range 303 - 1150 L), CL as 6.15 (range 2.41 - 18.7 L/h) and renal clearance as 0.587 (range 0.247 - 2.36). Inter-individual variability was estimated for V_1 , hepatic and renal clearance. Correlation between inter-individual variability of V_1 , hepatic and renal clearance was accounted for using an omega matrix. No relevant shrinkage in the omega distribution was observed (1.1% for V_1 , -0.3% for hepatic clearance and 9.6% for renal clearance).

Model validation

The adequacy of the approach to describe the effect of changes in protein-plasma concentration on the free fraction of solifenacin is shown in Figure 2. The AGP-plasma concentration is demonstrated to have a strong effect on f_u while the effect of albumin was shown to be negligible. This is in agreement with the roughly 1000 times lower partition coefficient observed for AGP (Table V) which overcomes the greater molar plasma concentration of albumin. As a consequence variation in AGP ends up playing a main role in the plasma binding of solifenacin.

Adequate description of the plasma and urine data by the model is illustrated by the internal visual predictive check (Figure 3). Slight model overprediction of the plasma concentrations is observed only for the control group of study 2

(Figure 3; upper left panel). The internal visual predictive check also illustrates that part of the inter-individual variability can be explained by considering only the variability in the physiological parameters, i.e. without random-effect (inner shade). For the urine data the variability in the physiological parameters (inner shade) can explain most of the inter-individual variability observed.

Extrapolations

Figure 4 and 5 illustrates the results of the visual predictive check performed to evaluate the predictive power of the semi-physiological approach for hepatic and renal impaired patients, respectively. In the liver impaired patients, the approach slightly overpredicts the terminal half-life of the observed total plasma concentrations while in renal impaired patients the observed total plasma concentrations is underpredicted, especially in the patients classified as severe and to a lesser extent in the patients classified as moderate (Figure 6; upper panel). Predictions substantially improved when the potential involvement of hepatic uptake transporters were taken into account by increasing the intrinsic clearance by a factor of 0.6 in patients with a GFR lower than 40 mL/min/1.73 m² (Figure 6; lower panel). The population prediction and the inter-individual variability did not markedly change when the model predictions were based on either the observed or literature reported alterations (Table III) of the physiological parameters (Figure 4 and 5).

Table VI illustrates the posterior predictive check results for V_{SS} , CL and renal clearance for liver impaired patients and mild, moderate and severe renal impaired patients. The median of the post hoc estimates were inside the 95% confidence interval of the posterior predictive distribution. For severe renal

impaired patients, the posterior predictive check results confirmed the improvements in the predictions observed after considering the potential involvement of hepatic uptake transporters.

Discussion

The application of model-based drug development in special populations becomes increasingly important for clinical trial optimization, mostly by providing rationale for dose selection and thereby aiding risk-benefit assessment. Currently, WB-PBPK models have been employed for prediction of the pharmacokinetics in patients with liver impairment (Edginton and Willmann 2008; Johnson *et al.* 2010). However, attempts to use this approach sometimes fail as WB-PBPK models require extensive knowledge on all active processes impacting the pharmacokinetics of the drug. As an alternative, a semi-physiological approach is proposed for pharmacokinetic extrapolations. This concept takes into account key principles from physiology in combination with the non-linear mixed effect modeling approach for estimation of population and random-effect parameters. In this paper, the semi-physiological concept is presented enabling the prediction of the pharmacokinetics from healthy subjects to patients under two different disease conditions, i.e., liver and renal impairment.

The uniqueness of this approach relies on the utilization of a general partitioning framework to account for binding to plasma proteins and to non-plasma tissues together with principles from physiology that apply to the main pharmacokinetic process (i.e., bioavailability, distribution and elimination). In combination with compartmental modeling, the proposed semi-physiological approach can be used to investigate the impact of (patho-) physiological alterations on the time course of drug concentration. An important feature of the proposed semi-physiological approach is that the model captures

physiological parameters that are believed to change under pathophysiological conditions. To this end, extrapolation of the pharmacokinetics from healthy volunteers to liver and renal impaired patients relies on the key principle that only the physiological parameters change without the need for adjustment of the model structure and/or pharmacokinetic parameter estimates.

In this investigation, solifenacin served as a model compound to show the validity of the concept. Rich clinical pharmacokinetic data of total solifenacin was available from healthy subjects and patients with liver and/or renal impaired function. In addition, free solifenacin in plasma and solifenacin in urine were included in the analysis. As solifenacin extensively binds to AGP, which is known to widely vary under liver and renal impaired conditions, it was anticipated that protein binding would be a physiological parameter of key relevance. Accordingly, solifenacin was considered a suitable model compound to investigate the utility of the proposed semi-physiological approach.

First, the semi-physiological approach was applied to characterize the pharmacokinetics of solifenacin in healthy subjects (Figure 1).

Characterization of the binding of solifenacin to plasma proteins in the model was a key step for the inclusion of the physiological principles which allowed investigation of the impact of key physiological parameters on the time course of solifenacin concentration. These key physiological parameters represented body composition, glomerular function, liver enzyme capacity and liver blood flow. In addition, inclusion of the physiological principles improved the

understanding of the pharmacokinetic properties of solifenacin by interpretation of model estimates. For example, the agreement between the model estimated bioavailability and the bioavailability obtained in a clinical study (Kuipers *et al.* 2004) indicate that bioavailability of solifenacin is mainly affected by the first-pass metabolism in the liver. Also, the 10 fold difference between the measured $CL_{in\text{ vitro}}$ (results not published) and the estimated $CL_{in\text{ vivo}}$ (0.00451 L/h/g liver protein; Table V) indicated the involvement of influx hepatic drug transporters promoting the *in vivo* hepatic clearance of solifenacin (Wu and Benet 2005)). This 10-fold difference is well above the average 5-fold difference that Hallifax *et al* demonstrated as not sufficient to support the role of hepatic transporters (Hallifax, Foster, and Houston 2010).

For the extrapolation of the pharmacokinetics of solifenacin to patients with hepatic and renal impairment, only the physiological parameters were adapted according to expected alterations as reported in the literature (Table III) or to the alterations observed in the patients included in the clinical trials (Table IV). Interestingly, the observed changes in physiological parameters are in good agreement with the values derived from the literature. Hence, the expected alterations as reported in the literature are deemed suitable for predictions of the pharmacokinetics under these disease conditions, except for albumin-plasma concentration in liver impaired patients whose reported differences of 0.68 (Table III) were not supported by the observed data which showed no differences (Table IV). Because solifenacin mainly binds to AGP, it is expected that the difference in albumin concentration has only minimal impact on the model performance. This is confirmed by the fact that the predictions using literature reported changes in the physiological parameters are

comparable to the predictions using the observed parameters (Figure 4). Therefore, the slight overprediction of the terminal half-life of liver impaired patients is rather caused by relative low number of patients included in this study and the cross-study differences in solifenacin concentrations also observed for the control group (Figure 3).

For predictions of the pharmacokinetic time course in renal impaired patients, alterations in CL were initially assumed to be limited to increased AGP concentration and decreased GFR. Evaluation of the predictions, as depicted in Table VI and Figure 5, indicates that imposing only these assumptions result in an underprediction of CL. Considering a decrease in the hepatic intrinsic clearance for renal impaired patients with a GFR lower than 40 mL/min/1.73m² resulted in a better prediction of CL (Figure 6 and Table VI). This alteration in hepatic clearance represents literature evidence that hepatic transporters are likely to be altered under renal impaired conditions (Nolin *et al.* 2008). The quantification of the potential changes in the activity of the hepatic uptake transporter appears to be independent of the type of the transporter involved and is in agreement with the hepatic clearance reductions reported by Dreisbach *et al.* (Dreisbach and Lertora 2003). The accuracy of these extrapolations also supports the role of hepatic transporters.

Additional evidence that hepatic transporters play a more prominent role than renal transport mechanisms is provided by the fact that the semi-physiological model adequately predicted the urine extraction ratio in liver and renal impaired patients (Table VI and Figure 5). In this respect, any potential reduction in the transporters involved in the active tubular secretion as

reported by Dreisbach *et al* (Dreisbach 2009) was not accounted for by the model. We believe however that further expansion of the semi-physiological model accounting for tubular secretion will not result in a further improvement of the predictions as only a small percentage of total-solifenacin is renally excreted.

Overall, application of the semi-physiological model to predict the time course of solifenacin concentration in renal and liver impaired patients shows that distribution of solifenacin is mainly driven by differences in f_u and intrinsic clearance and less by other key physiological variables that may change under disease conditions. For example, underestimation of body composition by the anthropometric equations (Himmelfarb *et al.* 2002;Proulx *et al.* 2005) did not influence the accuracy of the pharmacokinetic predictions (Table VI) in liver and renal impaired patients. For other populations, like obese patients, body composition may play a more prominent role than protein binding in the determination of the time course of drug concentration.

In conclusion, the proposed semi-physiological approach combines physiological principles with the non-linear mixed effect modeling allowing estimation of population and random-effect parameters. This allowed a better understanding of the pharmacokinetic properties of solifenacin. Moreover, the semi-physiological approach enables prediction of the time course of solifenacin concentration in liver and renal impaired patients by using *a priori* knowledge of changes in physiological parameters. To this end, the semi-physiological approach is instrumental for prediction of altered pharmacokinetics of compounds influenced by disease conditions.

Acknowledgments

This work was performed within the framework of the Dutch Top Institute Pharma project D2-104. The authors gratefully acknowledge Carla Santillan for her assistance in acquiring the data required for model development and extrapolation. No source of funding was used to assist in the preparation of this study. The authors have no conflicts of interest that are directly relevant to the contents of this study.

Authors contribution

Participated in research design: Strougo, A, Freijer, J, Danhof, M and
Krauwinkel, WJJ

Performed data analysis: Strougo, A

Wrote or contributed to the writing of the manuscript: Strougo, A, Yassen A,
Freijer, J

Reference list

- Boer P (1984) Estimated lean body mass as an index for normalization of body fluid volumes in humans. *Am. J Physiol*, **247**: F632-F636.
- Chouker A, Martignoni A, Dugas M, Eisenmenger W, Schauer R, Kaufmann I, Schelling G, Lohe F, Jauch KW, Peter K, Thiel M (2004) Estimation of liver size for liver transplantation: the impact of age and gender. *Liver Transpl.*, **10**: 678-685.
- Cockcroft DW, Gault MH (1976) Prediction of creatinine clearance from serum creatinine. *Nephron*, **16**: 31-41.
- Doroshenko O, Fuhr U (2009) Clinical pharmacokinetics and pharmacodynamics of solifenacin. *Clin Pharmacokinet.*, **48**: 281-302.
- Dreisbach AW (2009) The influence of chronic renal failure on drug metabolism and transport. *Clin Pharmacol Ther*, **86**: 553-556.
- Dreisbach AW, Lertora JJ (2003) The effect of chronic renal failure on hepatic drug metabolism and drug disposition. *Semin. Dial.*, **16**: 45-50.
- Edginton AN, Willmann S (2008) Physiology-based simulations of a pathological condition: prediction of pharmacokinetics in patients with liver cirrhosis. *Clin Pharmacokinet.*, **47**: 743-752.
- Gibaldi M, McNamara PJ (1978) Apparent volumes of distribution and drug binding to plasma proteins and tissues. *Eur. J Clin Pharmacol*, **13**: 373-380.
- Hallifax D, Foster JA, Houston JB (2010) Prediction of human metabolic clearance from in vitro systems: retrospective analysis and prospective view. *Pharm. Res.*, **27**: 2150-2161.
- Haycock GB, Schwartz GJ, Wisotsky DH (1978) Geometric method for measuring body surface area: a height-weight formula validated in infants, children, and adults. *J Pediatr*, **93**: 62-66.
- Himmelfarb J, Evanson J, Hakim RM, Freedman S, Shyr Y, Ikizler TA (2002) Urea volume of distribution exceeds total body water in patients with acute renal failure. *Kidney Int.*, **61**: 317-323.
- Janmahasatian S, Duffull SB, Ash S, Ward LC, Byrne NM, Green B (2005) Quantification of lean bodyweight. *Clin. Pharmacokinet.*, **44**: 1051-1065.

Johnson TN, Boussey K, Rowland-Yeo K, Tucker GT, Rostami-Hodjegan A (2010) A semi-mechanistic model to predict the effects of liver cirrhosis on drug clearance. *Clin Pharmacokinet.*, **49**: 189-206.

Johnson TN, Rostami-Hodjegan A, Tucker GT (2006) Prediction of the clearance of eleven drugs and associated variability in neonates, infants and children. *Clin. Pharmacokinet.*, **45**: 931-956.

Krauwinkel WJ, Smulders RA, Mulder H, Swart PJ, Taekema-Roelvink ME (2005) Effect of age on the pharmacokinetics of solifenacin in men and women. *Int. J. Clin. Pharmacol. Ther.*, **43**: 227-238.

Kuipers M, Smulders R, Krauwinkel W, Hoon T (2006) Open-label study of the safety and pharmacokinetics of solifenacin in subjects with hepatic impairment. *J. Pharmacol. Sci.*, **102**: 405-412.

Kuipers ME, Krauwinkel WJ, Mulder H, Visser N (2004) Solifenacin demonstrates high absolute bioavailability in healthy men. *Drugs R. D.*, **5**: 73-81.

Levey AS, Bosch JP, Lewis JB, Greene T, Rogers N, Roth D (1999) A more accurate method to estimate glomerular filtration rate from serum creatinine: a new prediction equation. Modification of Diet in Renal Disease Study Group. *Ann Intern Med*, **130**: 461-470.

Mehvar R (2005) Role of protein binding in pharmacokinetics. *Am. J. Pharm. Educ.*, **69**: 1-8.

Michel MC, Yanagihara T, Minematsu T, Swart PJ, Smulders RA (2004) Disposition and metabolism of solifenacin in humans. *Br. J. Clin. Pharmacol.*, **59**: 647.

Nolin TD, Naud J, Leblond FA, Pichette V (2008) Emerging Evidence of the Impact of Kidney Disease on Drug Metabolism and Transport. *Clin Pharmacol Ther*, **83**: 898-903.

Payne CK (2006) Solifenacin in overactive bladder syndrome. *Drugs*, **66**: 175-190.

Post TM, Freijer JI, Ploeger BA, Danhof M (2008) Extensions to the visual predictive check to facilitate model performance evaluation. *J Pharmacokinet. Pharmacodyn.*, **35**: 185-202.

Proulx NL, Akbari A, Garg AX, Rostom A, Jaffey J, Clark HD (2005) Measured creatinine clearance from timed urine collections substantially overestimates glomerular filtration rate in patients with liver cirrhosis: a systematic review

and individual patient meta-analysis. *Nephrol. Dial. Transplant.*, **20**: 1617-1622.

Rowland M, Tozer TN (1995) *Clinical Pharmacokinetics: Concepts and Applications*. Lippincott Williams & Wilkins.

Schuppan D, Afdhal NH (2008) Liver cirrhosis. *Lancet*, **371**: 838-851.

Simpson D, Wagstaff AJ (2005) Solifenacin in overactive bladder syndrome. *Drugs Aging*, **22**: 1061-1069.

Smulders RA, Smith NN, Krauwinkel WJ, Hoon TJ (2007) Pharmacokinetics, safety, and tolerability of solifenacin in patients with renal insufficiency. *J. Pharmacol. Sci.*, **103**: 67-74.

Vasson MP, Baguet JC, Arveiller MR, Bargnoux PJ, Giroud JP, Raichvarg D (1993) Serum and urinary alpha-1 acid glycoprotein in chronic renal failure. *Nephron*, **65**: 299-303.

Watson PE, Watson ID, Batt RD (1980) Total body water volumes for adult males and females estimated from simple anthropometric measurements. *Am. J Clin Nutr.*, **33**: 27-39.

Wu CY, Benet LZ (2005) Predicting drug disposition via application of BCS: transport/absorption/ elimination interplay and development of a biopharmaceutics drug disposition classification system. *Pharm. Res.*, **22**: 11-23.

Wynne HA, Cope LH, Mutch E, Rawlins MD, Woodhouse KW, James OF (1989) The effect of age upon liver volume and apparent liver blood flow in healthy man. *Hepatology*, **9**: 297-301.

Yang J, Jamei M, Yeo KR, Rostami-Hodjegan A, Tucker GT (2007) Misuse of the well-stirred model of hepatic drug clearance. *Drug Metab Dispos.*, **35**: 501-502.

Figure legends

Figure 1 Schematic representation of the semi-physiological model developed for solifenacin. The arrows within the central compartment represent instantaneous equilibrium and arrows between compartments represent kinetic processes. Total and free-solifenacin plasma concentrations as well as plasma-protein concentrations were measured in the compartments indicated by the bold lines and grey color. The urine concentration was measured in the compartment named urine.

Figure 2 Relationship between f_u and plasma-proteins. Open circles: observed data used for model development (control group study 1 and 2 and study 3); open triangles: observed data used for extrapolation (liver and renal impaired groups in study 1 and 2); line: population prediction (median); shade area: 95% confidence interval of the predicted median.

Figure 3 Internal visual predictive check of the total-solifenacin plasma concentrations (panels A and B) and urine (panels C and D) excretion rate after single (panels A and C) and multiple (panels B and D) doses administration of 5 and 10 mg o.d. of solifenacin. Open circles: observed data of study 1 and 3; open triangles: observed data study 2; line; population prediction (median); inner shade: 90% predicted population variability explained by the differences in the physiological parameters; outer shade: 90% predicted population variability including differences in the physiological parameters and random-effects.

Figure 4 Plasma (panels A and B) and urine (panels C and D) extrapolation results to patients with liver impairment. Panels A and C represent the extrapolations based on expected changes in the physiological parameters (Table III) and panels B and D represent extrapolations based on observed physiological parameters (Table IV). Open triangles: observed data study 2; line; population prediction (median); shade: 90% including differences in the physiological parameters and random-effects.

Figure 5 Plasma (panels A and B) and urine (panels C and D) extrapolation results for patients with renal impairment. Panels A and C represent the extrapolations based on expected changes in the physiological parameters and panels B and D represent extrapolations based on observed physiological parameters. Open circles: observed data mild impaired group; open triangles: observed data moderate group; crosses: observed data severe group; line; population prediction (median); shade: 90% including differences in the physiological parameters and random-effects.

Figure 6 Plasma extrapolation results for patients with renal impairment subclassified as mild, moderate and severe. All extrapolations were based on observed physiological parameters. The panels A, B and C represent the extrapolations with unchanged intrinsic clearance while the panels D, E and F represent the extrapolation where the intrinsic clearance was assumed to change by 0.6 in patients with a GFR lower than 40 mL/min/1.73 m². Open circles: observed data mild impaired group; open triangles: observed data

moderate group; crosses: observed data severe group; line; population
prediction (median); shade: 90% including differences in the physiological
parameters and random-effects.

Tables

Table I Overview of the clinical studies used for model development and for comparison with model predictions

Study number	Study description	Population	Treatment schedule	Dosage	No. of subjects	Sampling scheme	Ref.
1	Open label	Healthy subjects ¹ ; Patients with mild, moderate or severe renal disease ² (6/group)	Single oral dose	10 mg	24	Plasma: 1, 2, 3, 4, 5, 6, 8, 12, 16, 24, 48, 96, 120, 168, 216, 264, 312 and 360 h post-dose Urine: 0-12 and 12-24h	(Smulders <i>et al.</i> 2007)
2	Open label, tolerability and pharmacokinetics	Healthy subjects ¹ ; Patients with moderate hepatic impairment ² (8/group)	Single oral dose	10 mg	16	Plasma: 1, 2, 3, 5, 6.5, 8, 12, 24, 48, 72, 96, 132, 168 h post-dose Urine: 0-6, 6-12, 12-24, 24-48, 48-72, 72-96, 96-120, 120-144 and 144-168h	(Kuipers <i>et al.</i> 2006)
3	Open label, 2-period crossover pharmacokinetics	Healthy subjects ¹	Multiple oral dose (14 days per period)	5 mg 10 mg	47	Plasma: day 12, 13: pre-doses day 14: pre-dose, 1, 2, 3, 4, 5, 6, 8, 12, 24, 48, 96, 144, 192 and 240 h post-dose Urine: day 14: 0-24h	(Krauwinkel <i>et al.</i> 2005)

¹data used for model development; ² data used for comparison with model predictions

Table II Overview of the demographic covariates, physiological parameters, estimated and derived model parameters

Model input		Model output		
Demographic covariates	Physiological parameters	Estimated parameters	Derived parameter (primary)	Derived parameter (secondary)
-	C_{Alb}, C_{AGP}	k_{Alb}, k_{AGP}	f_u	$CL_R, CL_H, F, V_{SS}, V_1, Q$
weight	Q_H	$CL_{in vivo}$	CL_{int}	CL_H, F
gender, age and weight	Liver weight			
race, gender, age and creatinine	GFR	α	CL_R	
gender, weight and height	V_{plasma}	β	V_1	
gender, weight and height	V_{plasma}	f_{tissue}	V_{SS}	
gender, age, weight and height	V_{water}			

Table III Overview of the expected changes in the physiological parameters in liver and renal impaired patients as a fraction of the values in healthy subjects

Physiological parameters	Liver impaired (Edginton and Willmann 2008)	Renal impaired
C_{AGP}	0.56	1.4 (severe) (Vasson <i>et al.</i> 1993)
C_{Alb}	0.68	1
Q_H	0.65	1
CL_{int}	0.40	0.6 ¹ (severe) (Nolin <i>et al.</i> 2008)
GFR	0.70	uniform distribution according to classification as specified in the protocol (see clinical studies)

¹ assuming that hepatic transporters are involved in the metabolism of the compound

Table IV Summary statistics (median and range) of the physiological parameters in various pathological conditions.

Physiological parameter	Control n=61	Liver impaired n=8	Renal impaired (Mild) ¹ n=6	Renal impaired (Moderate) ¹ n=6	Renal impaired (Severe) ¹ n=6
C _{AGP} (mg/dL)	79.5 (54 - 138)	43.5 (30 - 70)	81 (74 - 126)	87.5 (67 - 132)	111 (83 - 166)
C _{Alb} (g/dL)	4.17 (3.6 - 4.95)	4.14 (2.53 - 4.23)	4.20 (3.7 - 4.3)	4.00 (3.8 - 4.6)	3.85 (2.9 - 4.3)
V _{plasma} (L) (Boer 1984;Janmahasatian <i>et</i> <i>al.</i> 2005)	3.43 (2.21 - 4.4)	3.51 (2.18 - 3.74)	3.4 (2.81 - 3.67)	3.52 (3.02 - 4.12)	3.27 (3.01 - 3.98)
V _{water} (L) (Watson <i>et al.</i> 1980)	41.1 (28.4 - 52.4)	41.3 (28.1 - 45)	39 (32.6 - 42.4)	43.2 (36 - 51.1)	39.4 (36.5 - 48)
Liver weight (g)	2070 (1690 - 2550)	1990 (1830 - 2420)	1800 (1550 - 2060)	2240 (1770 - 2520)	2100 (1880 - 2240)
GFR (mL/min/1.73m ²)	87.8 (66.1 - 124)	78.8 (64.9 - 85)	57.4 (37.1 - 79.5)	28.7 (21.8 - 54.8)	19.5 (11.4 - 28.6)

¹ GFR classification based on Cockcroft-Gault equation: mild (GFR>50 and <80 mL/min), moderate (GFR>30 and <50 mL/min) or severe (GFR<30 mL/min)

Table V Population parameter estimates including coefficient of variation (CV%) and median of the derived structural parameters including range (minimum-maximum), if applicable.

Structural estimated parameters	Value (CV %)
ka (/h)	0.304 (12)
Cl _{in vivo} (L/h/g liver protein)	0.00451 (6.4)
α	5.56 (8.1)
Q* (L/h)	1120 (20)
β	5810 (11)
f _{tissue}	0.00142 (4.6)
k _{AGP} (nmol/L)	659(18)
k _{Alb} (nmol/L)	293000 (22)
Structural derived parameters	Median (range)
F	0.93 (0.891 - 0.954)
V ₁ (L)	331 (165 - 982)
V ₂ (L)	161 (89.2 - 264)
V _{SS} (L)	484 (303 - 1150)
CL (L/h)	6.15 (2.41 - 18.7)
CL _H (L/h)	5.62 (2.11 - 16.3)
CL _R (L/h)	0.587 (0.247 - 2.36)
Q (L/h)	23.1 (15.6 - 29.7)
f _u	0.0205 (0.0139 - 0.0264)
Random inter-individual variability	Value (CV %)
ω ² V ₁	0.114 (20)
ω ² CL _H	0.163 (18)
ω ² CL _R	0.212 (19)
Residual error	Value (CV %)

σ^2 total	0.0181 (12)
σ^2 free	0.186 (83)
σ^2 urine	0.176 (30)

Table VI Posterior predictive check for V_{SS} , CL and renal clearance in various pathological conditions. For every pharmacokinetic parameter the first row depicts the median of the observed values (post hoc analysis) and the second row depicts the simulated median and the 95% confidence interval of the posterior distribution (N=1000). In the control group only data from study 01 and 02 was used.

Pharmacokinetic parameter	Control	Liver impaired	Renal impaired (Mild ¹)	Renal impaired (Moderate ¹)	Renal impaired (Severe ¹)
V_{SS} (L)	604 537 (451 - 664)	771 768 (532 - 1030)	447 499 (395 - 633)	582 614 (479 - 774)	474 479 (356 - 626)
CL (L/h)	7.76 6.75 (5.31 - 8.60)	6.24 4.48 (3.15 - 6.34)	4.17 5.50 (4.06 - 7.66)	3.72 6.74 (4.86 - 9.32)	3.00 5.24 (3.86 - 7.38)
			4.97 (3.43 - 7.01) ²	4.66 (3.05 - 7.20) ²	3.29 (2.25 - 4.87) ²
CL_R (L/h)	0.988 0.701 (0.513 - 0.990)	0.798 0.817 (0.525 - 1.26)	0.319 0.428 (0.265 - 0.653)	0.375 0.251 (0.152 - 0.432)	0.151 0.133 (0.0774 - 0.218)

¹ GFR classification based on Cockcroft-Gault equation; ² predictions assuming differences in CL_{int} for $GFR < 40$ mL/min/1.73m²

Figure 1

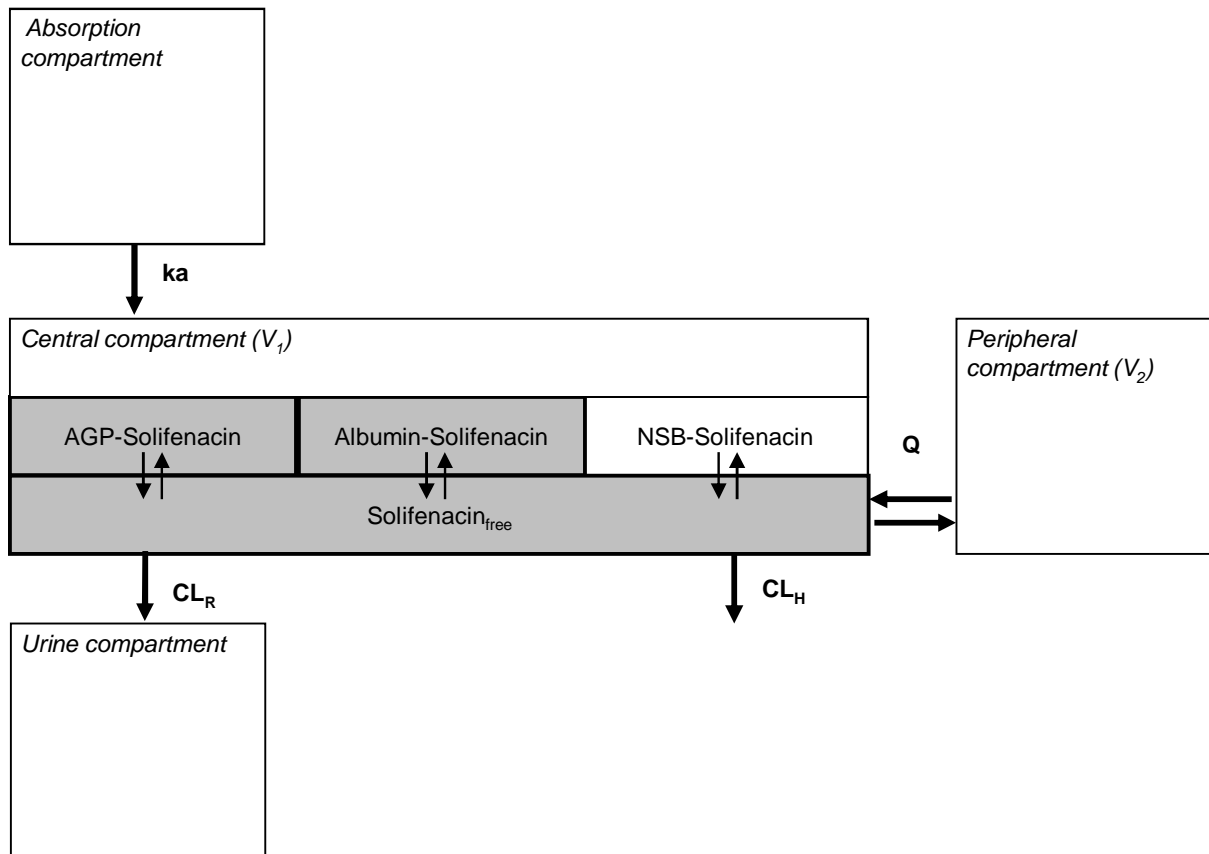


Figure 2

A

DMD #37838

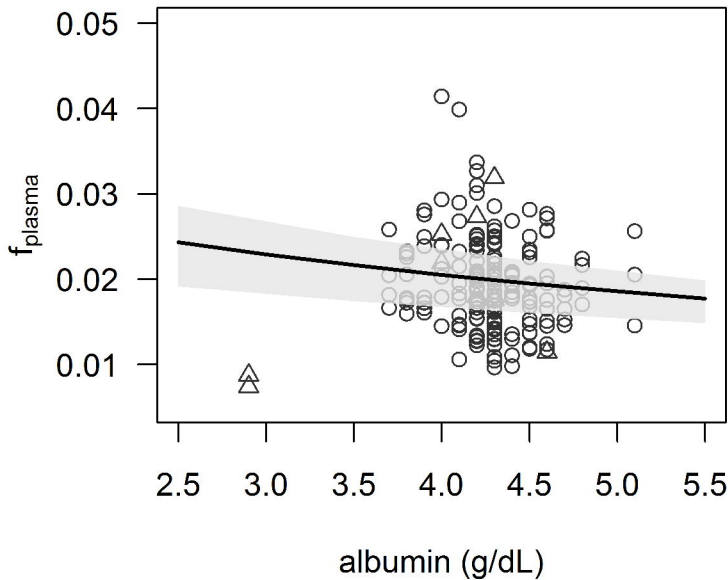
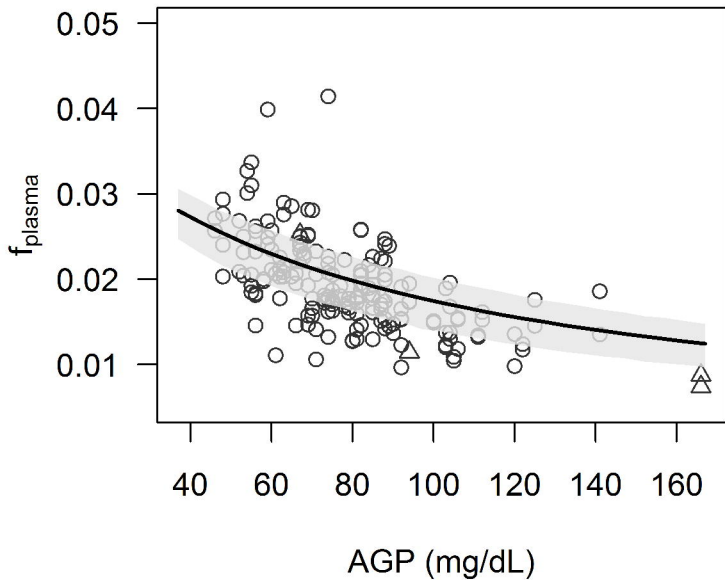
B

Figure 3

A single doses

DMD #37838

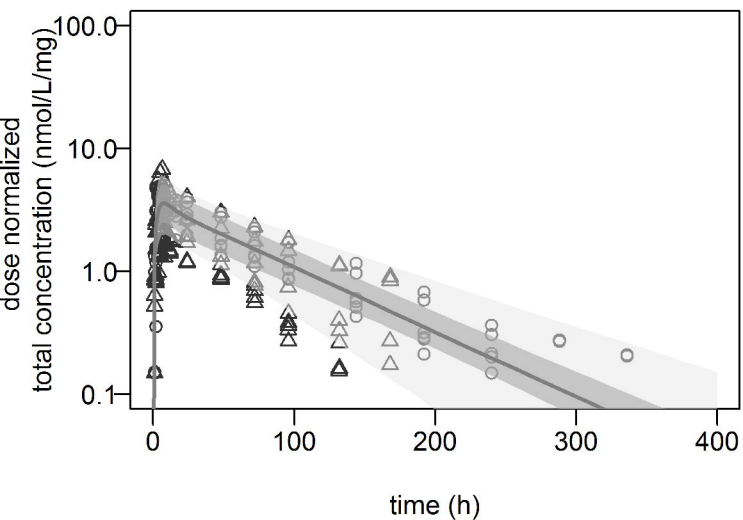
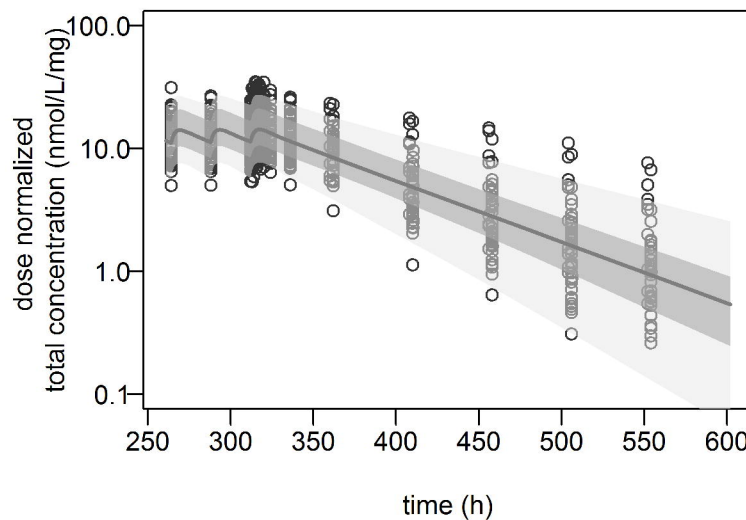
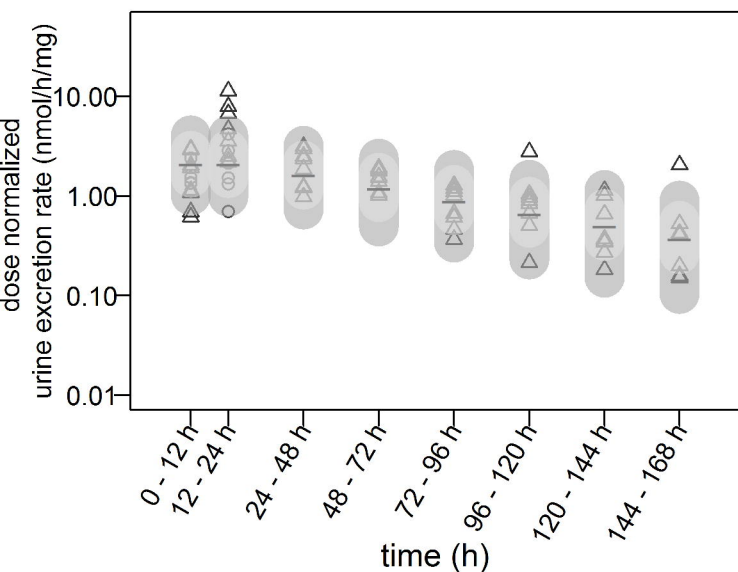
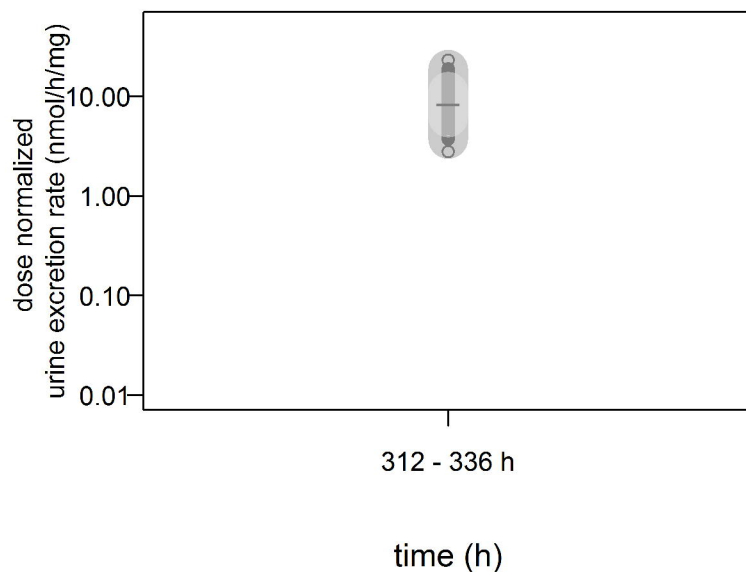
**B multiple doses****C single doses****D multiple doses**

Figure 4

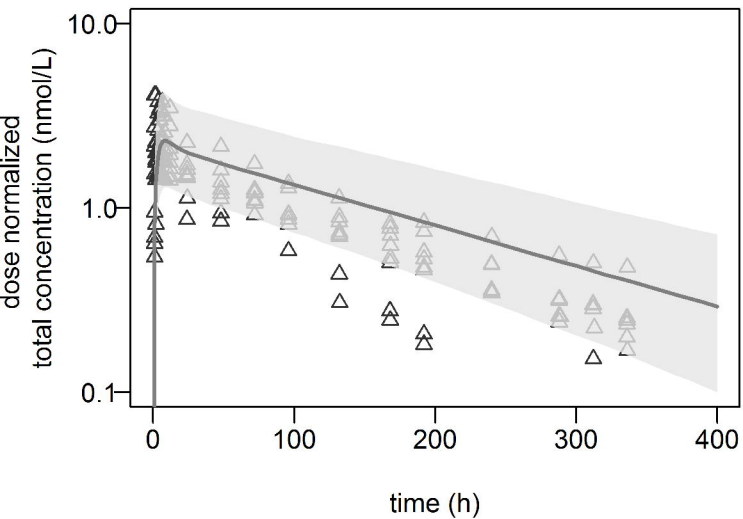
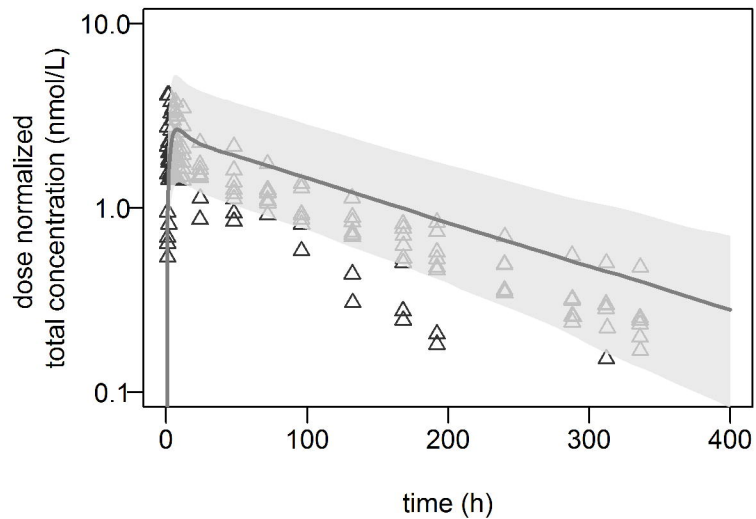
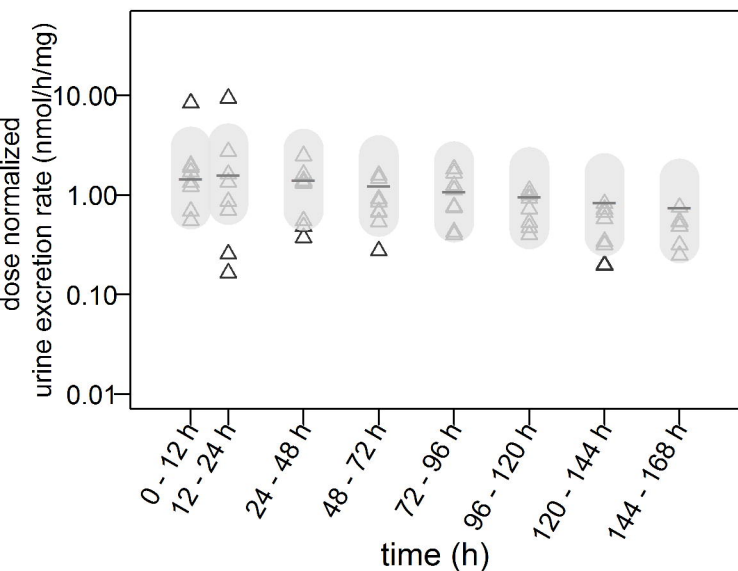
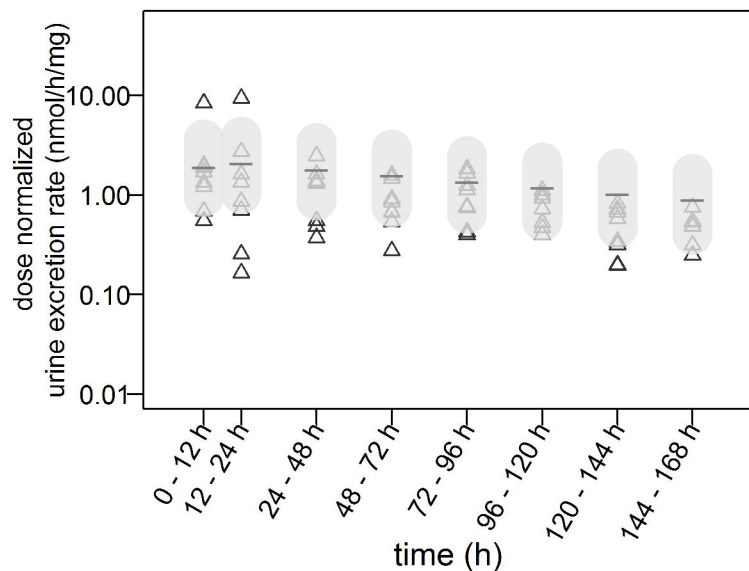
A**B****C****D**

Figure 5

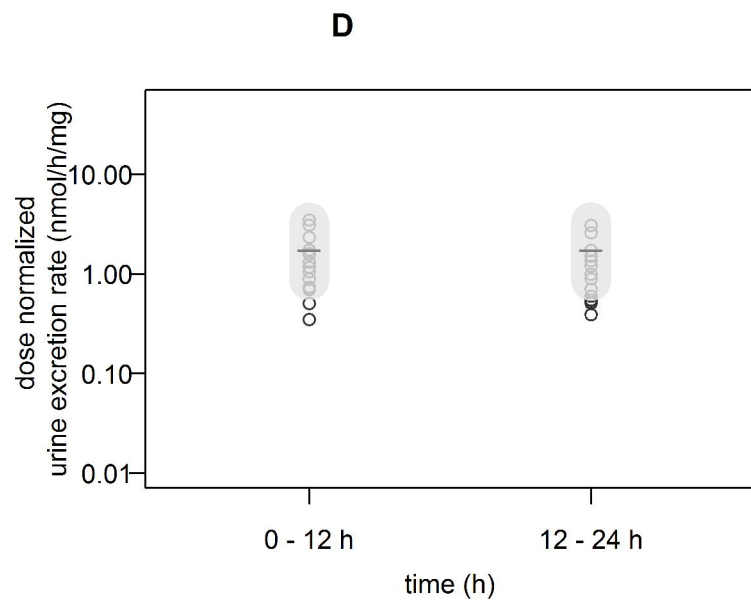
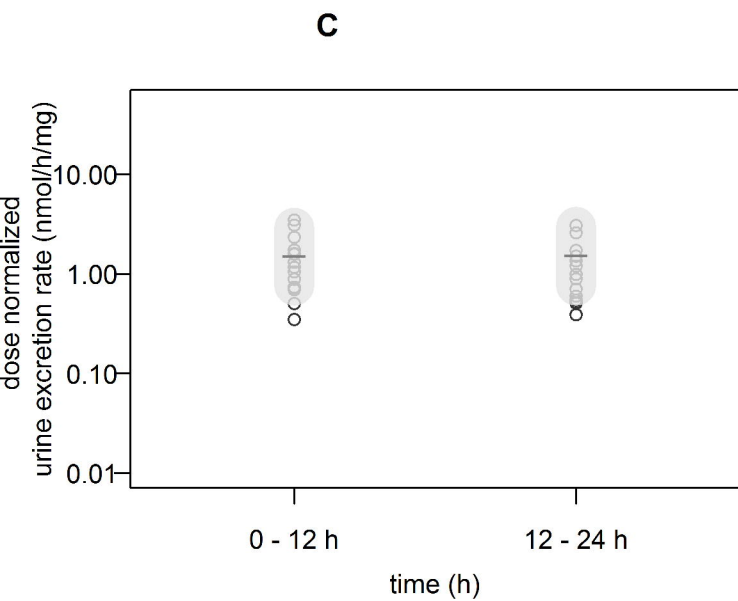
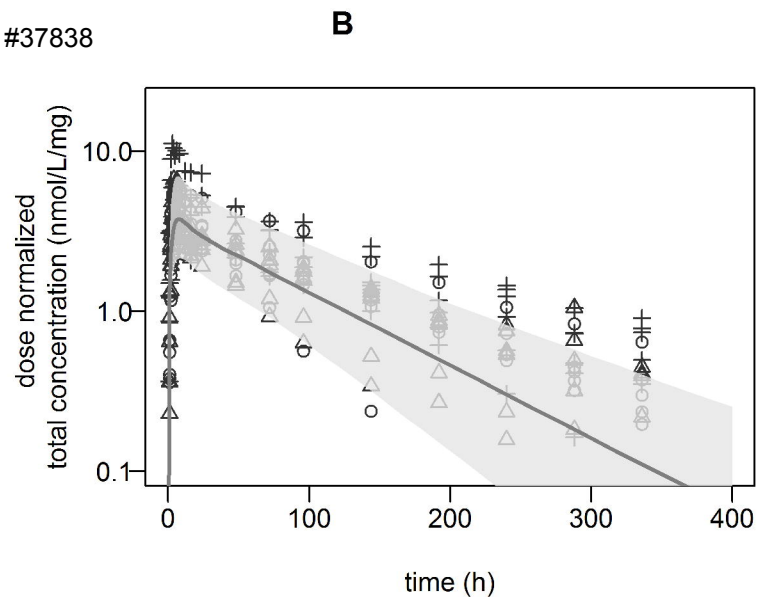
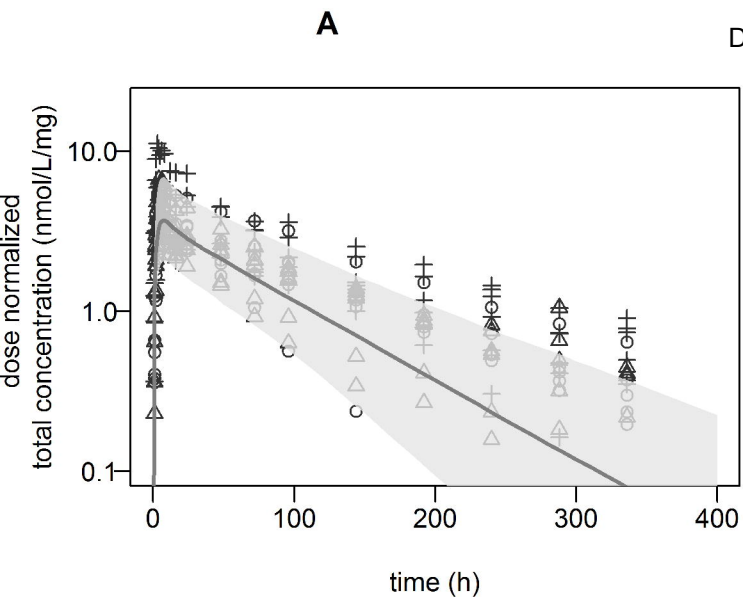
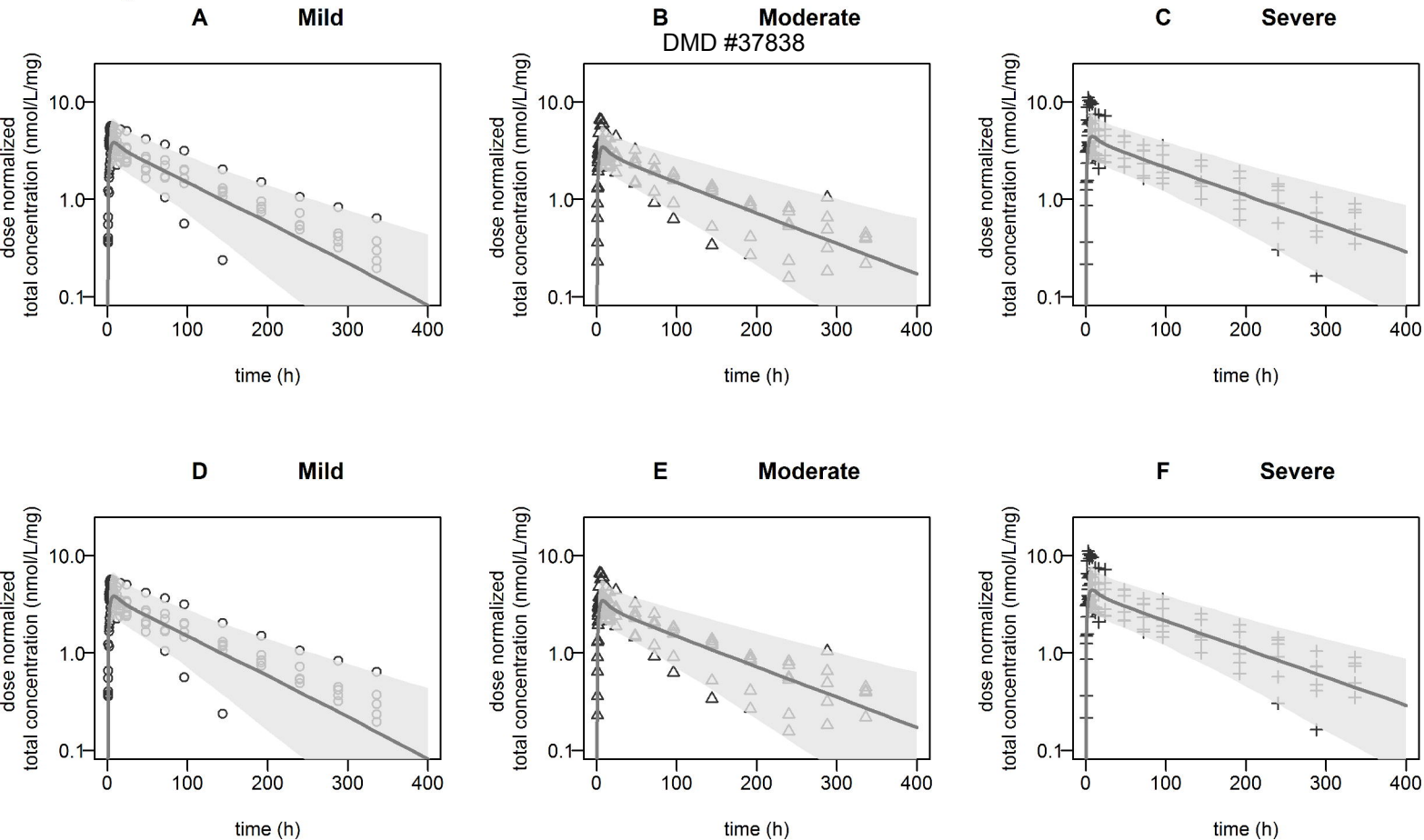


Figure 6

Correction to “A Semiphysiological Population Model for Prediction of the Pharmacokinetics of Drugs under Liver and Renal Disease Conditions”

In the above article [Strougo A, Yassen A, Krauwinkel W, Danhof M, and Freijer F (2011) *Drug Metab Dispos* 39:1278-1287], panels A, B, and C in Fig. 6 were duplicated as panels D, E, and F. The correct figure is given below.

The authors regret this error and apologize for any confusion or inconvenience it may have caused.

Figure 6

